Tidal-Traffic-Aware Routing and Spectrum Allocation in Elastic Optical Networks

Boyuan Yan, Yongli Zhao, Xiaosong Yu, Wei Wang, Yu Wu, Ying Wang, and Jie Zhang

***Abstract*—With the growing popularity of 5G mobile communications, cloud and fog computing, 4K video streaming, etc., population distribution and migration have increasing influence on traffic distribution in metro elastic optical networks (EONs). Traffic distribution is further diversified according to people's tendency to use network services in different places at different times. We use the term "tidal traffic" to represent traffic distribution with strong disequilibrium in the time and space dimensions. Note that tidal traffic can potentially result in low bandwidth utilization and weak service capability, as network resources are not allocated properly. To address this problem, in this study, we first analyze traffic characteristics of access networks and metro networks, and mathematically formulate an onion tidal traffic model (OTTM) in EONs. Second, based on the traditional routing and spectrum allocation (RSA) algorithm, which provides end-to-end connection by allocating frequency slot resources in EONs, we propose two algorithms to enhance bandwidth efficiency based on the OTTM model. We call them pre-detour RSA (PD-RSA) and pre-detour *k*-shortest paths RSA (PDK-RSA). Next, we analyze the shortcomings of a benchmark algorithm named min-hop *k*-shortest paths RSA (MHK-RSA) under tidal traffic, and compare PD-RSA and PDK-RSA with MHK-RSA via simulation. Simulation results show that PD-RSA and PDK-RSA can effectively reduce at least 26% and 18% of blocking probability, respectively, compared to MHK-RSA with the same time complexity.**

***Index Terms*—Elastic optical networks; Disequilibrium; Tidal traffic.**

I. Introduction

The tidal phenomenon, perceived as spatio-temporal fluctuation, is unavoidable in different networks such as transportation networks, the Internet, and social networks. Tidal traffic is caused mainly by the daily large-scale population migration among different areas at different times [1]. In general, traffic is usually more tidal in cities than in rural areas. In cities, some areas, depending on how busy they are throughout the day, e.g., business area/residential area, can experience traffic peaks and traffic valleys alternately. For example, in cities like Beijing, New York, or London, business areas are peak areas, and residential areas are valley areas during office hours (06:00–18:00), as most people are at work in business areas during this period. However, during off time (18:00–24:00 and 00:00–06:00), business areas are valley areas, and residential areas are peak areas, as during that time most people are at home.

Moreover, in tidal traffic, patterns can usually be found on traffic types in different types of areas. For example, high-bandwidth entertainment traffic demands, such as high-definition video and online games, may be primary network traffic sources in residential areas, while intercompany transaction and intracompany communication mainly make up the traffic in business areas. Most traffic demands from both residential and business areas are high-bandwidth demands served by wired connection. In contrast, most traffic demands on commute routes (bus, subway, etc.) are low-bandwidth demands served by wireless connections. All the traffic generated by users will be transmitted through access networks at first, then aggregated to metro networks, and forwarded to backbone networks, and finally transmitted to their destination. So, the disequilibrium of tidal traffic exists in any cross-area networks.

Generally, tidal traffic could result in inefficient network resource usage, as resources remain static as opposed to dynamic bandwidth requirements. Moreover, as the total traffic volume increases, the negative impact of inefficient network resource usage brought by tidal traffic is enlarged for traditional business and emerging business, such as virtual optical networks [2]. A Cisco Visual Networking Index (VNI) white paper [3] indicates that the global IP traffic will grow at a compound annual growth rate of 24% from 2016 to 2021. The VNI also shows that busy hour Internet traffic increased 51% in 2016, and will increase by a factor of 4.6 between 2016 and 2021, while average Internet traffic will increase by a factor of 3.2. The VNI [4] indicates that monthly global mobile data traffic will be 49 exabytes by 2021, which captures a significant portion of tidal traffic, and annual traffic will exceed half a zettabyte.

Some existing research with a focus on tidal traffic studied the resource-management problem in mobile networks

Manuscript received July 9, 2018; accepted July 26, 2018; published September 4, 2018 (Doc. ID 338232).

B. Yan, Y. Zhao (e-mail: yonglizhao@bupt.edu.cn), X. Yu, W. Wang, and J. Zhang are with the State Key Laboratory of Information Photonics and Optical Communications, Beijing University of Posts and Telecommunications, Beijing, China.

Y. Wu is with the University of California, Davis, California 95616, USA.

Y. Wang is with State Grid Information & Telecommunication Company, Beijing, 100761, China.

https://doi.org/10.1364/JOCN.10.000832

and access networks. Li *et al.* [5] proposed an energy-saving scheme over predicted traffic loads for tidal phenomenon in radio access networks. Sun *et al.* [6] proposed an intelligent SDN framework for 5G heterogeneous networks, which meets the dynamic nature of services and requirements. Troia *et al.* [7] proposed a collective non-negative-matrix factorization-based model to identify tidal traffic patterns in metro-area mobile networks. For WDM networks, Zhong *et al.* [1] proposed an online traffic-aware intelligent differentiated lightpath allocation algorithm to accommodate dynamic tidal traffic in IP-over-WDM networks. Alvizu *et al.* [8] proposed a suite of meta-heuristics to reduce energy consumption in mobile metro-core networks, while providing $1+1$ protection to aggregated traffic. Alvizu *et al.* [9] also solved an optical routing and wavelength assignment optimization problem by using tidal traffic variations predicted by machine-learning algorithms. For elastic optical networks (EONs), Klinkowski *et al.* [10] proposed three spectrum allocation schemes under time-varying spectrum requirements, and efficient heuristic algorithms to solve the multi-hour routing and spectrum allocation (RSA) problem. Ramaprasad *et al.* [11] proposed continuous-time and non-continuous-time heuristics to solve the routing, spectrum, and segment allocation problem.

RSA is a key functionality [12] to improve resource utilization in an EON. It does so by finding an appropriate route for a source and destination pair, and allocating suitable frequency slots (FSs) to the requested lightpath by following the continuity constraint and the contiguity constraint [13]. It is proved that RSA is an NP-complete problem [14], and many heuristic algorithms have been proposed to solve this problem in different scenarios. Jinno *et al.* [15] presented frequency slots based on the International Telecommunication Union (ITU-T) fixed grids for the first time, where the central frequency is 193.1 THz. Patel *et al.* introduced an efficient survivable network design algorithm [16], and proposed the spectrum defragmentation problem as a key sub-problem of RSA in EONs together with two heuristic algorithms [17]. Takagi *et al.* [18] further evaluated disruption-minimized spectrum defragmentation, which adopts distance adaptive modulation.

The studies mentioned above to address the inefficient resource utilization problem on tidal traffic lack a mathematical model to formulate traffic characteristics, thus making it hard to evaluate their performance in other networks and scenarios. In addition, the works on RSA rarely aim at a tidal traffic scenario. In this paper, for the first time to our knowledge, we propose an onion tidal traffic model (OTTM) to formulate tidal traffic in EONs. OTTM divides traffic into several parts according to peak-area location in the space dimension, and we use trigonometric functions to simulate the traffic change in the time dimension. Second, we propose a pre-detour strategy for RSA on the assumption that future traffic distribution could be known or predicted accurately. Third, we propose two algorithms, which we have named the pre-detour RSA (PD-RSA) algorithm and the pre-detour k-shortest paths RSA (PDK-RSA) algorithm to reduce blocking probability. Compared with the benchmark min-hop k-shortest paths RSA (MHK-RSA), PD-RSA, and PDK-RSA consider hop count, present traffic distribution, and trend of traffic distribution of tidal traffic, and result in lower blocking probability with the same time complexity.

The rest of the paper is organized as follows. Section II presents OTTM and a traffic generation method. Section III introduces the MHK-RSA algorithm, PD-RSA, and PDK-RSA. Section IV shows numerical results. Section V concludes our study.

II. Tidal Traffic Formulation

A. Onion Tidal Traffic Model

In this section, we formulate OTTM to model the tidal traffic [19,20]. Figure 1 shows a metro EON consisting of 28 optical nodes and 52 fiber links. It was divided into residential and business areas, circled by solid and dashed lines, respectively. During office hours, the business area is the peak area and he residential area is the valley area. During off time, the business area becomes the valley area and the residential area becomes the peak area. Thus, the boundary between the peak area and the residential area follows the boundary between the business area and the residential area. However, in some cases, the business area contains not only office buildings, but also some residential districts, and residential districts can also be used for business purposes. This indicates the boundary between business areas and residential areas is not deterministic. Figure 2 shows a more reasonable tidal traffic distribution during office hours. Traffic intensity peaks at the core of business area and fades as distance from the peak increases, as illustrated by the darkness level in Fig. 2.

However, a metro EON is usually used to aggregate traffic, and its number of nodes is usually lower than an access network. After aggregation, traffic intensity on the EON topology should be discrete. Based on this, we propose OTTM to describe tidal traffic distribution in EONs. As shown in Fig. 3, the whole network is divided into several parts from inside to outside during office hours in OTTM. O_0 carries the heaviest traffic load, which is the core surrounded by several annuluses. Traffic loads in different annuluses are different from each other, and decrease from O_1 to O_3 in a step-wise fashion. The shape of Fig. 3 resembles an onion with O_0 being the onion core.

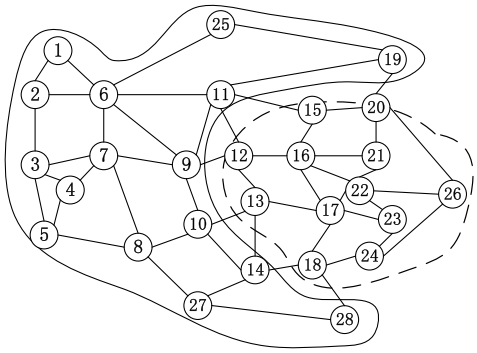

Fig. 1. Business and residential areas in a metro optical network.

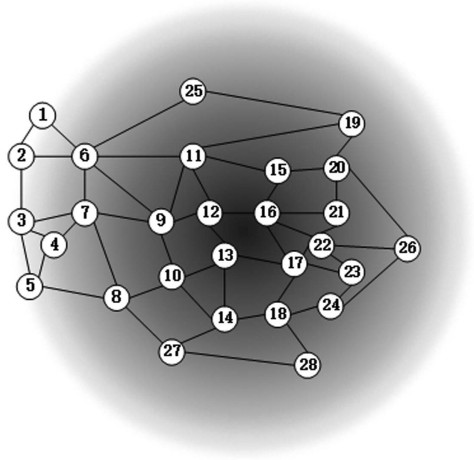

Fig. 2. Smooth transition of traffic load in a metro optical network.

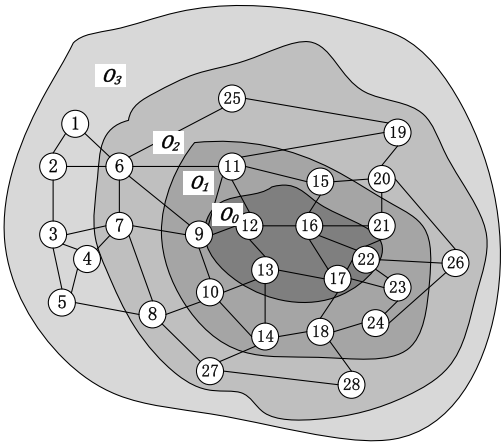

Fig. 3. Diagram of OTTM.

To simplify, we assume that there is only one business area and one residential area where traffic distribution layouts for office and off time hours are similar, as [1] did. This means that there is also an onion core and several onion skins during off time in another district.

To formulate OTTM, we define some variables as follows:

- $G(V,E)$: EON topology, where V is a set of nodes, and E is a set of fiber links.
- v_i: the ith node in V.
- e_{ij}: the link between v_i and v_j $(i<j)$.
- O_l: the node set of the lth circle area. In Fig. 3, the network has been divided into four circle areas:
  - $O_0=\{v_{12},v_{13},v_{16},v_{17},v_{22}\}$
  - $O_1=\{v_9,v_{10},v_{11},v_{14},v_{15},v_{18},v_{21},v_{23},v_{24}\}$
  - $O_2=\{v_6,v_7,v_8,v_{19},v_{20},v_{25},v_{26},v_{27},v_{28}\}$
  - $O_3=\{v_1,v_2,v_3,v_4,v_5\}$
- ρ_{bias}: arrival rate for stable random connections. The stable connections are those connections that are not affected by population migration. The arrival rate could follow a stochastic generation model, such as a Poisson process.
- m: number of annuluses in OTTM. In Fig. 3, $m=3$.
- ρ_l: l denotes the area index with different arrival rates, ρ_l denotes the arrival rates of local peak connections whose source and destination are both in set $\{O_0,O_1,\ldots,O_l\}$ apart from $\rho_{\text{bias}},\rho_0,\ldots,\rho_{l-1}$. For example, ρ_0 denotes the arrival rate of set $\{O_0\}$ apart from ρ_{bias}, ρ_1 denotes arrival rate of set $\{O_0,O_1\}$ apart from ρ_{bias} and ρ_0, and so on in a similar fashion. That fashion of traffic superposition is similar to a tower of Hanoi, as Fig. 4 shows.
- t_s: start time of the peak.
- t_e: end time of the peak.

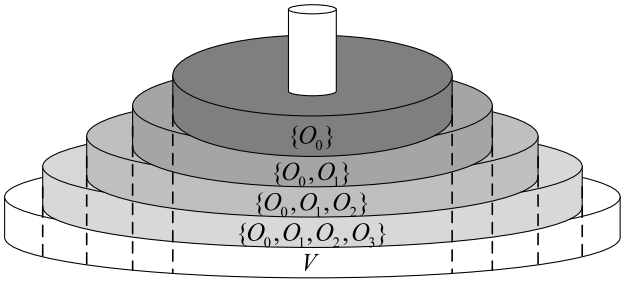

Fig. 4. Traffic superposition of a single peak under OTTM.

B. Tidal Traffic Generation

According to population migration in one day, arrival connections of tidal traffic on the topology in Figs. 1–3 could be divided into three categories:

i) **Stable random connections**: the connections whose arrival rate is ρ_{bias}. It could be considered a base line for tidal traffic.

ii) **Local business peak connections**: the connections generated by $\rho_0,\rho_1,\rho_2,\rho_3$, which contribute to the peak in office hours on top of stable random connections.

iii) **Local residential peak connections**: similar with local business peak connections, but O_0 locates on the core of the residential area.

As Fig. 5 shows, the dashed line represents network capability. The bars in three colors indicate the traffic loads for stable random, local business peak, and local residential peak connections at different periods of the day. The total traffic load on an optical node in a metro optical network is the sum of stable random traffic and residential peak traffic during office time, or the sum of stable random traffic and business peak traffic in office hours. Congestion occurs when the bar is higher than the dashed line. Local business/residential peak connections contribute the most to network congestion. We assume there is no mutual effect between the business peak traffic and the residential peak traffic so that we can focus on the times within a single peak (one time tidal) instead of a whole day. This paper uses time-varying Poisson arrival rate ρ (min^{-1}) with fixed

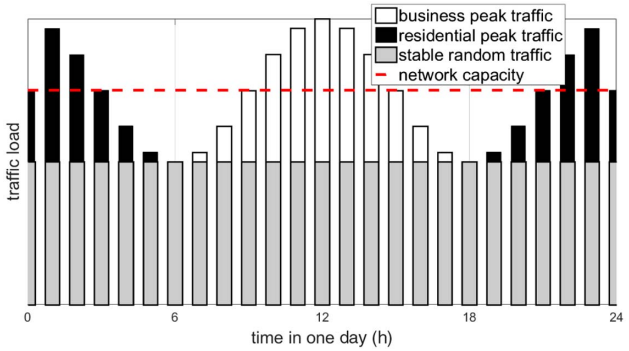

Fig. 5. Traffic load variation in one day.

negative exponential holding times μ (min^{-1}) to describe traffic flow.

The equations to define $\rho_l(t)$ are as follows

$$\rho_0 = \rho_{\text{bias}}, \qquad t \in [t_s, t_e], \tag{1}$$

$$\rho_l(t) = \rho_l\left[1 + \sin\left(\frac{2\pi}{t_d}(t - t_s) - \frac{\pi}{2}\right)\right], \quad l \in [1, m], \quad t \in [t_s, t_e]. \tag{2}$$

In Eq. (2), we use trigonometric sines [21] to simulate the trend of tidal traffic. The connection generator can be built once $\rho_{\text{bias}}, \rho_0, \ldots, \rho_m$ and other variables are set.

III. Tidal-Traffic-Aware RSA Algorithms

In this section, first, we define some global variables to describe the problem. Second, we analyze shortcomings of the MHK-RSA algorithm. We then propose two tidal-traffic-aware algorithms. Finally, we evaluate the time complexity of the proposed algorithms.

A. Problem Statement

RSA is a key problem in EONs. RSA is used to calculate routes for traffic demands and allocate flexible frequency slots to build lightpaths. The RSA problem involves two basic constraints: the continuity constraint and the contiguity constraint. The former ensures that the allocated spectral resources are the same along the links in the route, and the latter guarantees that those resources are contiguous in the spectrum area. In this paper, MHK-RSA is a benchmark algorithm that is unaware of traffic trends. The proposed heuristic algorithms are aware of the trend of tidal traffic through effective methods such as machine-learning algorithms. To describe these algorithms in detail, the following variables and functions are defined:

- S: total available slot number of each optical link.
- $C(v_s, v_d, r, t_b, t_o)$: a connection request, where v_s is the source node, v_d is the destination node, r is the required slot number, t_b is the begin time, and t_o is the time when C is over.
- CQ: connections queue, in which connections are sorted in ascending order of arrival time.
- T: period that can be predicted from now.
- $ew_{i,j}$: edge weight of $e_{i,j}$.
- HEW: set of all $ew_{i,j}$ with $ew_{i,j} = 1.0$, $\forall e_{i,j} \in E$.
- PEW: set of all $ew_{i,j}$ according to current and future traffic distributions.
- $R_{i,j}$: calculated available path set from source node v_i to destination node v_j.
- $r_{i,j}$: one available path of $R_{i,j}$.
- $rw_{i,j}$: route weight of path $r_{i,j}$.
- $c_{i,j}$: occupied slots number on edge $e_{i,j}$ currently.
- $f_{i,j}$: occupied slots number on edge $e_{i,j}$ in the future within T.
- TC: current traffic load distribution on $G(V,E)$, that is, $TC = \{c_{i,j} | e_{i,j} \in E\}$.
- TF: future traffic load distribution on $G(V,E)$, that is, $TF = \{f_{i,j} | e_{i,j} \in E\}$.

B. Greedy and Pre-Detour Algorithms

1) *MHK-RSA Algorithm*: MHK-RSA is a greedy algorithm, a benchmark to handle network congestion in EONs. MHK-RSA calculates k-shortest paths by using Yen's algorithm [22], and checks if the spectrum resources of these paths can satisfy the continuity constraint and the contiguity constraint. If these constraints are satisfied, MHK-RSA will select the best path to set up the connection. The RSA for the connection is selected according to the shortest path (in terms of hop count) with enough spectrum available, whereas the slot is selected using first-fit.

MHK-RSA is able to exploit the spectrum potentialities in networks. However, there are still two key shortcomings if being applied to tidal traffic. First, most of spectrum resources in a high-load area would be allocated in advance while traffic tide is raising. This will cause high blocking probability for those connections whose source/destination nodes are in a high-load area and influence the connections, which have to go through high-load area. In Fig. 6, the bold red lines denote the high-load optical links, and it is hard to reach the nodes surrounded by red lines, e.g., v_{13}. Second, blocking in the high-load area would make many connections bypass the high-load area to avoid failures. Bypassing increases hop count, and thus costs more spectrum resources. If these connections are established successfully, spectrum resources in the surrounding areas will be exhausted. An example in Fig. 6 shows four calculated alternative paths (Table I) for a connection with source node v_7 and destination node v_{16}. If there are not enough spectrum resources for a min-hop path, the remaining paths will be chosen. The chosen path is longer, costs more spectrum resources, and reduces bandwidth capacity of each link of itself.

2) *PD RSA Algorithm*: PD-RSA is designed to overcome those two shortcomings of MHK-RSA. In PD-RSA, we consider not only hop count, but also current traffic distribution and

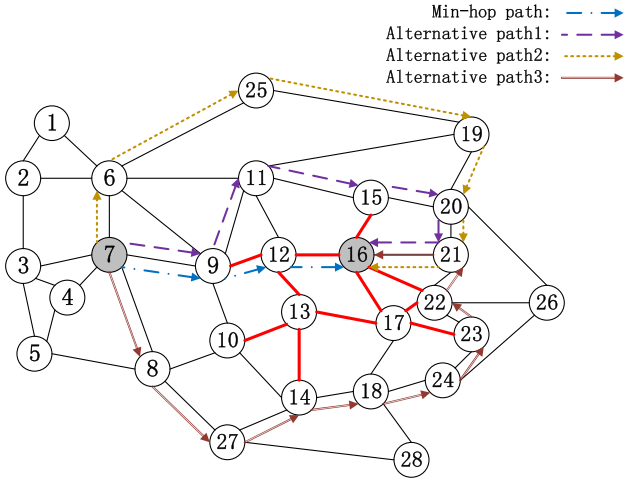

Fig. 6. Multiple paths from v_7 to v_{16}.

TABLE I
ALTERNATIVE PATHS SUMMARY

Path Name	Route	HOP COUNT
Min-hop path	$v_7 \to v_9 \to v_{12} \to v_{16}$	3
Path 1	$v_7 \to v_9 \to v_{11} \to v_{15} \to v_{20} \to v_{21} \to v_{16}$	6
Path 2	$v_7 \to v_6 \to v_{25} \to v_{19} \to v_{20} \to v_{21} \to v_{16}$	6
Path 3	$v_7 \to v_8 \to v_{27} \to v_{14} \to v_{18} \to v_{24} \to v_{23} \to v_{22} \to v_{21} \to v_{16}$	9

future traffic trends jointly. The pseudo code of PD-RSA is shown in Algorithm I.

Algorithm 1: PD-RSA Algorithm

1. $t \leftarrow 0$, initialize TF for time $t+T$, TC for time t, and PEW.
2. **For** connection $C(v_s, v_d, r, t_b, t_o)$ in CQ **Do**
3. **If** $t_b \geq t+T$ **Then**
4. $t \leftarrow t+T$
5. update TF for time $t+T$
6. update TC for time t_b
7. calculate PEW according to TC and TF.
8. **End If**
9. calculate shortest path $sr_{s,d}$ based on *HEW*.
10. calculate traffic distribution-based path based on *PEW*.
11. **If** both $sr_{s,d}$ and can provide bandwidth r **Then**
12. $\Delta hc \leftarrow$ difference between hops of $tr_{s,d}$ and hops of $sr_{s,d}$
13. $\Delta si \leftarrow$ difference between minimum available spectrum slot index of $tr_{s,d}$ and of $sr_{s,d}$
14. **If** $\Delta hc == 0$ **Then**
15. $br_{s,d} \leftarrow tr_{s,d}$
16. **Else If** $\Delta hc \leq th$ **Then**
17. **If** Δhc is larger than product of r_t and hops of $sr_{s,d}$ **Then**
18. $br_{s,d} \leftarrow sr_{s,d}$
19. **Else If** Δsi is not more than product of r_s and minimum available spectrum slot index of $tr_{s,d}$ **Then**
20. $br_{s,d} \leftarrow tr_{s,d}$
21. **Else**
22. $br_{s,d} \leftarrow sr_{s,d}$
23. **End If**
24. **Else**
25. $br_{s,d} \leftarrow sr_{s,d}$
26. **End If**
27. **Else If** only one of $\{sr_{s,d}, tr_{s,d}\}$ can provide bandwidth r **Then**
28. set satisfied one as $br_{s,d}$
29. **Else**
30. C is blocked
31. **End If**
32. choose route $br_{s,d}$ and execute resource allocation
33. **End For**

At the beginning of PD-RSA, we obtain the traffic distribution p_{result} after time T from now, and repeat this process after every T. When a connection $C(v_s, v_d, r, t_b, t_o)$ arrives, we calculate two paths, and choose the better one to execute resource allocation. One path is the shortest min-hop route $\text{sr}_{s,d}$ calculated by Dijkstra's algorithm based on HEW. The other path is the traffic-distribution-based route $\text{tr}_{s,d}$ calculated by Dijkstra's algorithm based on PEW. Because traffic load changes with time, we set PEW according to traffic distributions in the time dimension

$$ew_{i,j} = c_{i,j} + \alpha \cdot f_{i,j}, \quad \forall\, ew_{i,j} \in \text{PEW}. \tag{3}$$

Here, α indicates the importance of current and future traffic distributions. The larger is α, the higher is the importance of future traffic distribution.

To select a path $\text{br}_{s,d}$ from $\{\text{sr}_{s,d}, \text{tr}_{s,d}\}$, we introduce th, r_t, and r_s to measure a path. th is the threshold of the hop difference between $\text{tr}_{s,d}$ and $\text{sr}_{s,d}$. r_t is the threshold of the ratio of hop difference to hop count of $\text{sr}_{s,d}$. r_s is the threshold of the ratio of the FS-index difference between $\text{tr}_{s,d}$ and $\text{sr}_{s,d}$ to the FS-index of $\text{sr}_{s,d}$.

First, th and r_t are two limitations about hop count, which indicates that if $\text{tr}_{s,d}$ uses too many more spectrum resources than $\text{sr}_{s,d}$, it cannot be considered a good choice, if $\text{hops}(\text{tr}_{s,d}) - \text{hops}(\text{sr}_{s,d}) > \text{th}$ or $\frac{\text{hops}(\text{tr}_{s,d}) - \text{hops}(\text{sr}_{s,d})}{\text{hops}(\text{sr}_{s,d})} > r_t$. Thus, $\text{sr}_{s,d}$ is considered a better choice. Second, the minimum available slot index to be allocated to C is also a key factor that reflects spectrum compactness and resource occupation. If the ratio of FS-index of these two paths exceeds r_s, traffic load on $\text{tr}_{s,d}$ is high, and *vice versa*. Finally, according to the comparisons mentioned above, we can draw a conclusion about which one is better.

3) PDK-RSA Algorithm: In PD-RSA, we obtain two paths that are easy to implement, but it is hard to guarantee their high performance in some scenarios. Increasing the number of calculated paths is a feasible way to improve PD-RSA. In PDK-RSA, as shown in Algorithm II, we replace Dijkstra's algorithm by Yen's algorithm to calculate k traffic distribution-based paths, and put them into set TR at Step 4. TR is a set of $\text{tr}_{s,d}$ in PD-RSA. Then, we compare $\text{sr}_{s,d}$ with each one of TR (Steps 12–26) in PD-RSA,

and choose the first one that is better than $\mathrm{sr}_{s,d}$. If all *TR*s are worse than $\mathrm{sr}_{s,d}$, $\mathrm{sr}_{s,d}$ will be the final choice.

Algorithm 2: PDK-RSA Algorithm

```
1.  t ← 0, initialize TF for time t + T, TC for time t, and PEW.
2.  For connection C(v_s, v_d, r, t_b, t_o) in CQ Do
3.    the same as Steps 3-9 of Algorithm I
4.    calculate k traffic distribution-based paths based on PEW, put them into set TR.
5.    check if every r_{s,d} ∈ TR can provide bandwidth r, and filter the mismatched out of TR.
6.    If sr_{s,d} is unable to provide bandwidth r Then
7.      If TR is empty Then
8.        C is blocked
9.      Else
10.       br_{s,d} ← the path with the min-hop count, min-available slot index in TR.
11.     End If
12.   Else
13.     If TR is empty Then
14.       br_{s,d} ← sr_{s,d}
15.     Else
16.       sort elements of TR in hop-count ascending order
17.       For every tr_{s,d} ∈ TR Do
18.         the same as Step. 12-26 of Algorithm I
19.         If br_{s,d} == tr_{s,d} Then
20.           Break
21.         End If
22.       End For
23.     End If
24.   End If
25.   choose route br_{s,d} and execute resource allocation
26. End For
```

C. Time-Complexity Analysis

In this subsection, we analyze the time complexity of the MHK-RSA, PD-RSA, and PDK-RSA algorithms.

1) *Time Complexity of MHK-RSA*: The time complexity depends mainly on the cost of calculating k-shortest loop-less paths and the cost of finding an available slot index. As proved by Bouillet [23], the time complexity of path calculation using Yen's algorithm is $O(k|V|(|E|+|V|\log|V|))$. S slots will be searched on each link of every path. Since the path is loop-less, its hop count is $|V|-1$ at most. Thus, the time complexity of MHK-RSA is

$$\begin{aligned} T_{\mathrm{MHK}} &= O(k|V|(|E|+|V|\log|V|)) + O(k\cdot S(|V|-1)) \\ &= O(k|V|(S+|E|+|V|\log|V|)). \end{aligned} \tag{4}$$

Moreover, when k equals 1, Dijkstra's algorithm could be used to replace Yen's algorithm. As proved by Fredman and Tarjan [24], the time complexity of Dijkstra's algorithm is $O(|E|+|V|\log|V|)$, so the time complexity of MHK-RSA ($k=1$) is

$$\begin{aligned} T_{\mathrm{MHK}} &= O(|E|+|V|\log|V|) + O(S(|V|-1)) \\ &= O(S|V|+|E|+|V|\log|V|)). \end{aligned} \tag{5}$$

2) *Time Complexity of PD-RSA*: There is a hidden loop at Steps 5–7 in Algorithm I to update *TF*, *TC*, and PEW on $|E|$ edges. This loop will be triggered every other $|T|$. If $|T|$ is small enough, this loop is triggered for each arrival connection. Dijkstra's algorithm has been used twice at Step 9 and Step 10, so the time complexity of PD-RSA to handle a connection is

$$\begin{aligned} T_{\mathrm{PD}} &= 2\cdot O(|E|+|V|\log|V|) + O(3|E|) + 2\cdot O(S(|V|-1)) \\ &= O(S|V|+|E|+|V|\log|V|). \end{aligned} \tag{6}$$

3) *Time Complexity of PDK-RSA*: In PDK-RSA, Dijkstra's algorithm is used to calculate the min-hop path, and Yen's algorithm is used to calculate k traffic distribution-based paths. Thus, the time complexity of PDK-RSA is

$$\begin{aligned} T_{\mathrm{PDK}} &= O(k|V|(|E|+|V|\log|V|)) + O(|E|+|V|\log|V|) \\ &\quad + O(3|E|) + (k+1)O(S(|V|-1)) \\ &= O(k|V|(S+|E|+|V|\log|V|)). \end{aligned} \tag{7}$$

IV. Numerical Evaluation

In this section, we conduct simulations on the network topology shown in Fig. 3. Apart from PD-RSA and PDK-RSA, we implement MHK-RSA as a benchmark.

We set the total number of spectrum slots as 100 per fiber link, and the negative exponential holding times of connections μ as 1 min^{-1}. The range of prediction period T is from 10 to 90 min. The range of prediction period T is from 10 to 90 min. The value of μ means 95% of the connection will last for 3 min, according to negative-exponential-distribution attributes. The scenario in which μ is much less than T is aimed at avoiding effects of elephant connections.

We use the onion traffic generator described in Eq. (2) to generate layered connections, and the annulus areas are the same as in Fig. 3. We set th as 2, r_t as 0.34, and r_s as 0.2. We set the arrival rate sequence $\{\rho_0,\rho_1,\rho_2,\rho_3\}$ in descending order, and the step value of traffic loads in adjacent circles equals 10, as

$$\rho_3 = \rho_2 - 10 = \rho_1 - 20 = \rho_0 - 30. \tag{8}$$

We set ρ_{bias} to 140 to indicate the Poisson stream of stable random connections. For each connection $C(v_s,v_d,r,t_b,t_o)$, the required number of slots r is an integer chosen randomly from [1,3]. t_s is set as 6, and t_e is set as 18.

We compare MHK-RSA and PD/PDK-RSA with k from 1 to 10. In all conditions, the performance of PD/PDK-RSA is better than MHK-RSA. The gap between them with the same k decreases while k increases. In order to convey the message in a clearer way, we skip some results with larger k.

A. MHK versus PD/PDK

Figure 7 shows the comparisons among MHK-RSA ($k = 1, 2, 3$), PD-RSA ($\alpha = 0.8$), and PDK-RSA ($\alpha = 0.8$, $k = 2, 3$) from 06:00 to 18:00 when a peak happens in the business area, under $T = 30$ min and $\rho_0 = 60$ min^{-1}. The blocking probability is measured every half-hour. As we observe, the trend of blocking probability follows the trend of traffic generation shown in Eq. (2). This implies that the tidal phenomenon cannot be eliminated no matter what algorithms are used. Blocking probabilities of MHK-RSA decrease gradually when k increases from 1 to 3. Furthermore, PD-RSA performs better than MHK-RSA ($k = 3$) at all peak times, but worse than PDK-RSA. This indicates that the traffic distribution-based path calculation can improve network performance. PDK-RSA ($k = 3$) performs better than PDK-RSA ($k = 2$), but the difference is small. This indicates that two implementations have similar service capability. In summary, the result proves that current and future traffic distribution information can indeed contribute to routing optimization in a time window, and that the number of calculated alternative paths has direct impact on blocking probability.

Figure 8 shows the comparisons among MHK-RSA ($k = 1, 2, 3$), PD-RSA ($\alpha = 0.8$), and PDK-RSA ($\alpha = 0.8$, $k = 2, 3$) under $T = 30$ min and different ρ_0. All six lines indicate blocking probability on various algorithms, and they are on the rise as load increases. Blocking probabilities are lower if k is larger in MHK-RSA and PDK-RSA, and blocking probabilities of PDK-RSA are lower than blocking probabilities of MHK-RSA.

Figure 9 shows the blocking probability reduction of PD/PDK compared with MHK. These three curves decrease as traffic load increases, and intersect each other when $\rho_0 = 55$, because the performance gap between MHK and PD-RSA(PDK-RSA) becomes smaller when traffic load increases with the same k. On lower traffic load, PD-RSA (PDK-RSA) is more efficient with larger k, but less efficient on higher traffic load. This is because there are fewer allocation choices when traffic load increases. The improvement on blocking probability decreases when traffic load increases, but it is always larger than 18%.

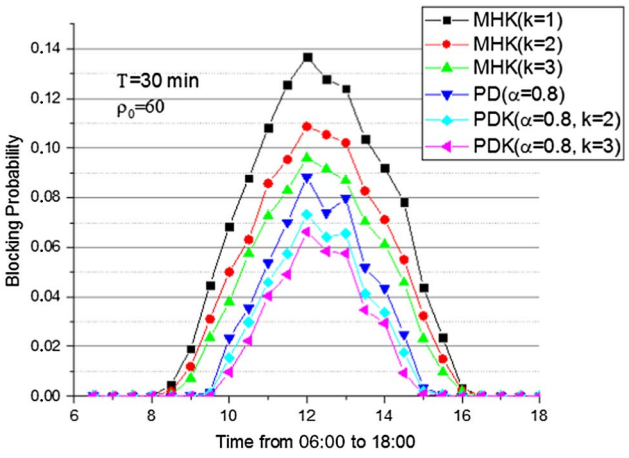

Fig. 7. Time-varying blocking probability in a business area.

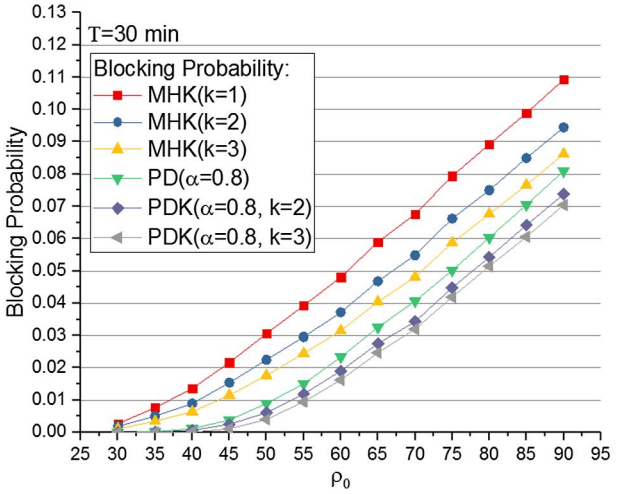

Fig. 8. Total blocking probability under different traffic loads.

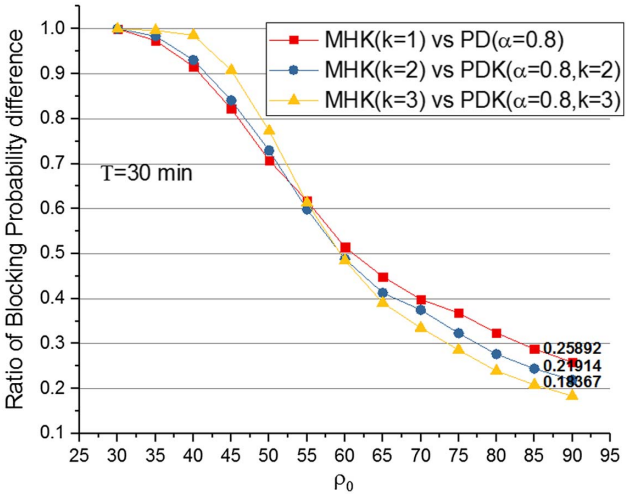

Fig. 9. Blocking probability improvement of PD/PDK compared with MHK.

B. Effects of α

Figure 10 shows the influence of α from 06:00 to 18:00 for PD-RSA, PDK-RSA ($k = 2$), and PDK-RSA ($k = 3$). The influences of α on these three algorithms are similar, because the key difference between PD-RSA and PDK-RSA is the number of alternative routes, and α is a factor to change edge weights for adjusting path calculation. The lines of $\alpha = 0$ in Figs. 10(a)–10(c) are higher than the other three lines. This indicates that it is necessary to consider the future trend of traffic distribution when $\rho_0 = 60$. There is similar performance among lines when $\alpha = 0.4/0.8/1.2$, which means in the condition where $\alpha >= 0.4$, α has little impact on performance improvement. α is a coefficient to measure the

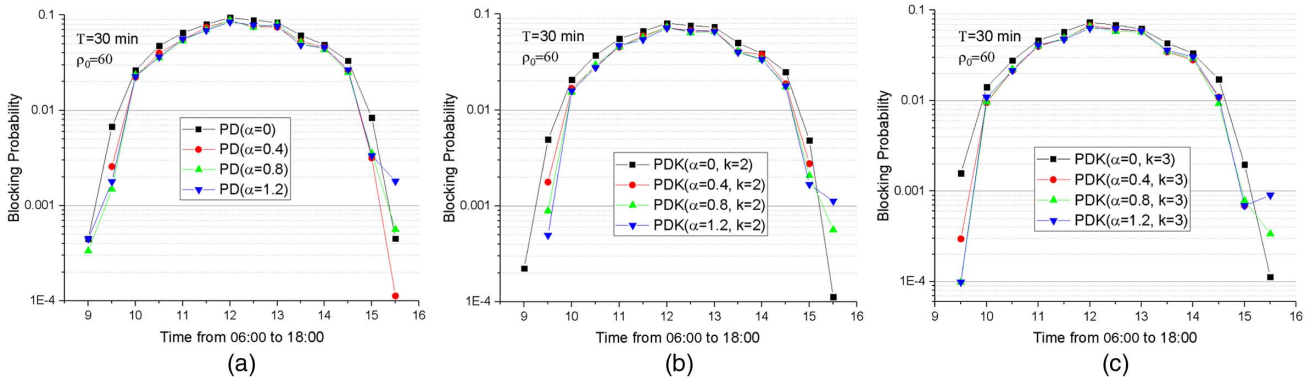

Fig. 10. Time-varying blocking probability with different α with different algorithms: (a) PD, (b) PDK ($k = 2$), and (c) PDK ($k = 3$).

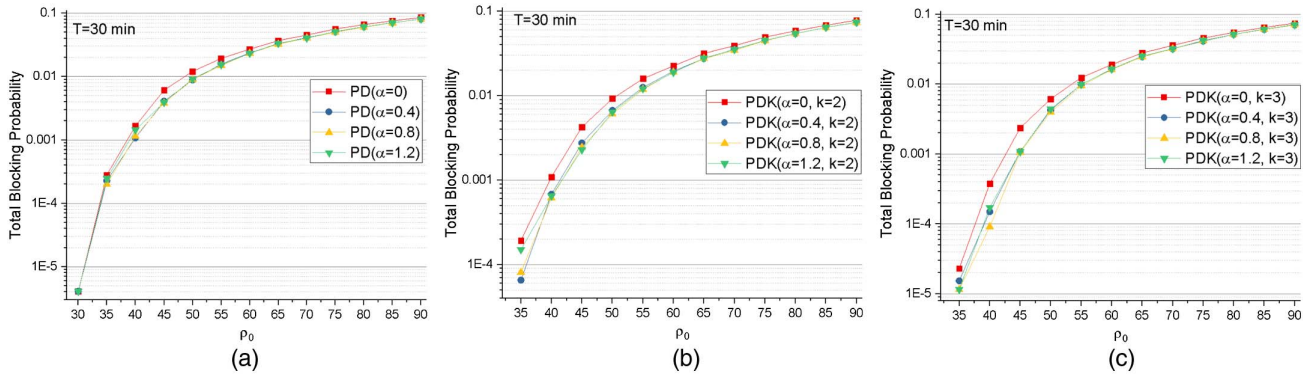

Fig. 11. Total blocking probability under different traffic load with different α with different algorithms: (a) PD, (b) PDK ($k = 2$), and (c) PDK ($k = 3$).

importance between current and future traffic distribution. Once α is big enough, the calculated paths will not change.

The upper line marked by squares is easy to distinguish from the other three lines in Fig. 11. In other words, blocking probability when $\alpha = 0$ is higher than that when $\alpha = 0.4/0.8/1.2$. This indicates the preference of considering future trend jointly over considering current traffic distribution only. One should reserve spectrum resources for coming connections when total blocking probability is lower than 10%.

C. Effects of Path Selection

At Steps 12–26 in PD-RSA and Step 18 in PDK-RSA, there is a path selection process between $\mathrm{sr}_{s,d}$ with min-hop count and $\mathrm{tr}_{s,d}$ calculated according to current and future traffic distribution. Figure 12 shows the influence of k, α, and ρ_0 for this process.

Figure 12(a) depicts the ratio of chosen $\mathrm{tr}_{s,d}$ to all successful connections with $\mathrm{tr}_{s,d} \neq \mathrm{sr}_{s,d}$. Figure 12(b) depicts the ratio of routes to all successful connections with $\mathrm{tr}_{s,d=}\mathrm{sr}_{s,d}$. The ratio in Fig. 12(a) always decreases, but in Fig. 12(b) it maintains growth while ρ_0 increases. That means the difference between $\mathrm{tr}_{s,d}$ and $\mathrm{sr}_{s,d}$ becomes small, especially when there are multiple choices for $\mathrm{tr}_{s,d}$ in PDK-RSA. When k is larger, the probability that $\mathrm{tr}_{s,d=}\mathrm{sr}_{s,d}$ is higher, because there are more alternative $\mathrm{tr}_{s,d}$ to match better routes, and the min-hop route is considered a good choice when traffic load is high. α impacts $\mathrm{tr}_{s,d}$ directly. It is helpful to find better routes for future traffic, so α is larger, the ratio in Fig. 12(a) is higher, and the ratio in Fig. 12(b) is lower. However, the sum of the ratios in Figs. 12(a) and 12(b) is always close to 100%, which means route decision depends on $\mathrm{tr}_{s,d}$ to a great extent.

D. Effects of T

T is crucial to impact prediction accuracy while using machine-learning algorithms or other prediction algorithms. The influence of stochastic noise and other factors reduce prediction precision when T is set improperly. Hence, the flexibility for T is required for applying a prediction. Figure 13 shows T's impact on PD-RSA with $\alpha = 0.8$, where T is set from 10 to 360 min. As the four subgraphs show, blocking probability reaches the minimal (MIN) when $T = 10$ min, and the maximum (MAX) when $T = 360$ min. The four dashed red horizontal lines indicate the blocking probability that is set as the border to keep performance stable; its value is 10% of (MAX-MIN) larger than MIN,

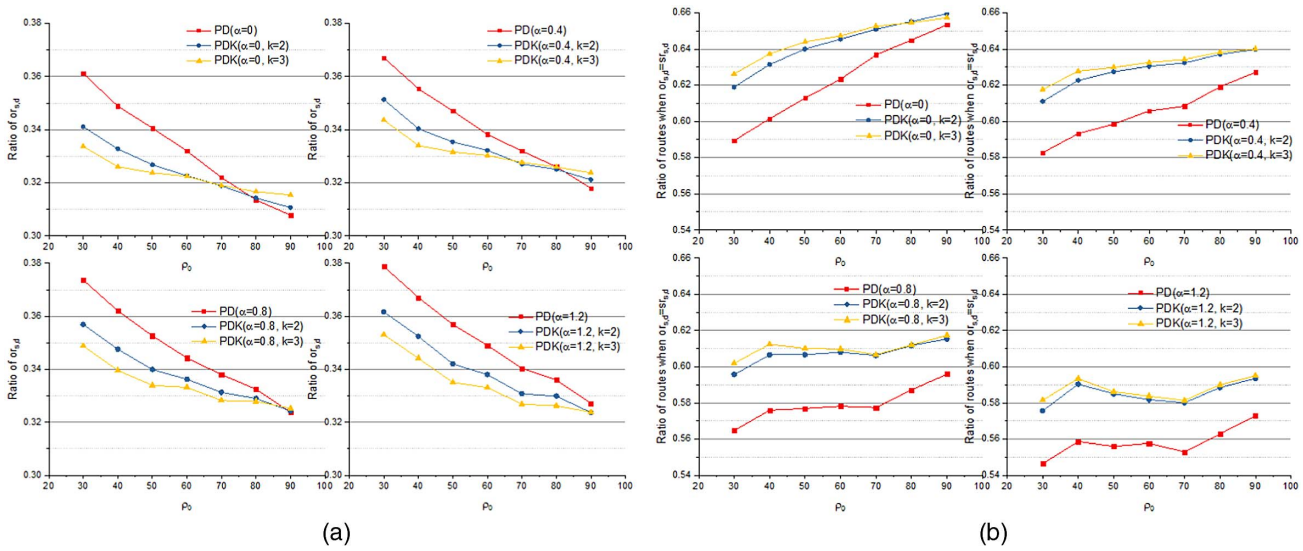

Fig. 12. Path selection about (a) ratio of $\mathrm{tr}_{s,d}$ to successful connections with $\mathrm{tr}_{s,d} \neq \mathrm{sr}_{s,d}$; (b) ratio of routes with $\mathrm{tr}_{s,d} = \mathrm{sr}_{s,d}$ to successful connections.

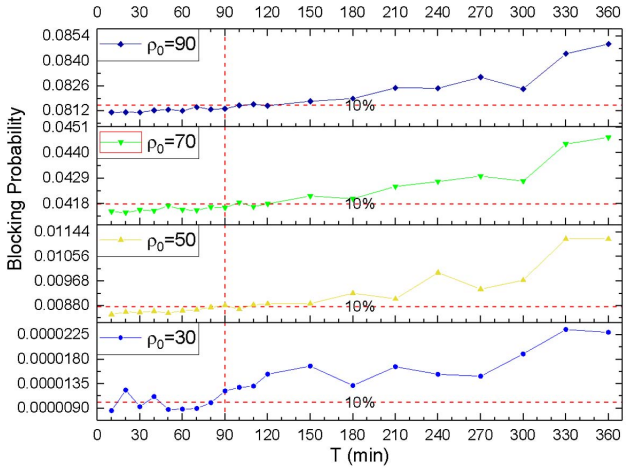

Fig. 13. Comparison under different T.

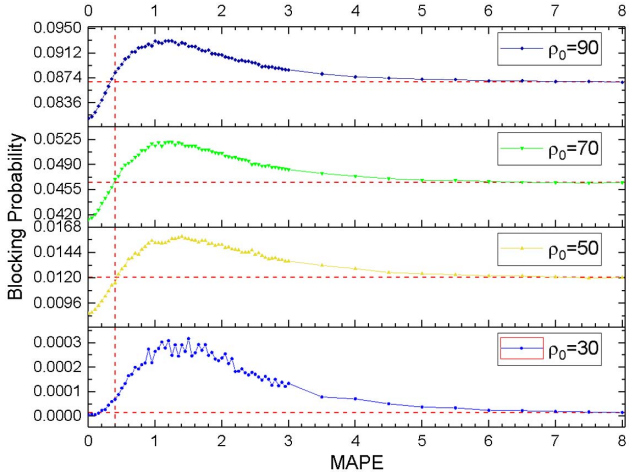

Fig. 14. MAPE influence on blocking probability.

i.e., $\mathrm{MIN} + 10\% \cdot (\mathrm{MAX} - \mathrm{MIN})$. According to the dashed red vertical line, we could see that the best value of T should be less than 90 min, or there would be performance cracking.

E. Effects of MAPE

All the results mentioned before are under the assumption that future traffic distribution can be predicted perfectly by using machine-learning or other algorithms. However, 100% accuracy of prediction is very hard for most predicting algorithms. To observe the influence of prediction accuracy, we introduce mean absolute percentage error (MAPE), a standard metric used to measure the accuracy of a prediction method in statistics. We assume that the occupied slots on link $e_{i,j}$ in real traffic distribution are $t_{i,j}$, thus, the MAPE of this prediction can be formatted as

$$\mathrm{MAPE} = \frac{100}{|E|} \sum_{e_{i,j} \in E}^{|E|} \left| \frac{t_{i,j} - f_{i,j}}{t_{i,j}} \right|. \tag{9}$$

We set MAPE from 0 to 8, which renders an accuracy range from 100% to 92%. In simulation, we use uniform distribution $u(\bullet)$ to approach predicted traffic under MAPE

$$f_{i,j} = t_{i,j} \times \left(1 + u(\{-1, +1\}) \times u\left(\left[0, \frac{\mathrm{MAPE}}{50}\right]\right)\right). \tag{10}$$

In Eq. (10), $u(\{-1, +1\})$ returns a random discrete value from set $\{-1, +1\}$ uniformly, and $u([0, \frac{\mathrm{MAPE}}{50}])$ returns a random continuous value between $[0, \frac{\mathrm{MAPE}}{50}]$ uniformly.

Figure 14 shows the influence of prediction accuracy under different MAPE. Any inaccuracy would cause degradation of the selected path, hence decreasing the efficiency of resource allocation. However, blocking probability

TABLE II
COST TIME OF PD-RSA AND PDK-RSA

Algorithm	Run Time (s)	Difference between k and $k-1$ (s)
PD-RSA	9.51	–
PDK-RSA ($k=2$)	628.89	619.38
PDK-RSA ($k=3$)	836.17	207.29
PDK-RSA ($k=4$)	1059.36	223.19
PDK-RSA ($k=5$)	1261.80	202.44
PDK-RSA ($k=6$)	1444.10	182.30
PDK-RSA ($k=7$)	1632.12	188.02
PDK-RSA ($k=8$)	1826.70	194.58
PDK-RSA ($k=9$)	2012.79	186.09
PDK-RSA ($k=10$)	2215.42	202.63

reaches its maximum when MAPE equals about 1.2, and then falls to a stationary value. The reason is that prediction becomes interference information when MAPE is larger than 1.2, and path selection is gradually able to offset part of the negative effects of prediction inaccuracy. The four dashed red horizontal lines represent the final stationary value of blocking probability. Before the maximum of the curves in Fig. 14, the blocking probability of each subgraph increases to the stationary value at about MAPE = 0.4. Therefore, to always make the performance good enough, MAPE should be less than 0.4, and the smaller the better.

F. Running Time

Although we have discussed the time complexity of the proposed algorithms, there are still some factors that we do not mention. Evaluation of running time for our simulation is necessary. As Table II shows, runtime increases with k, and the difference between PDK-RSA and PD(K-1)-RSA remains around 200 s, indicating a linear relation between them. There is a large gap between PD-RSA and PDK-RSA ($k=2$), which is explained in the complexity analysis of Eqs. (6) and (7).

V. CONCLUSION

In this paper, we focus on RSA efficiency improvement for tidal traffic. We propose a new tidal traffic pattern named OTTM in an EON. Then, a greedy algorithm to handle the RSA problem is introduced. We analyze its shortcomings for tidal traffic. Two heuristic algorithms, PD-RSA and PDK-RSA, are proposed to solve the problem. Simulation results show the proposed algorithms are efficient to reduce blocking probability.

ACKNOWLEDGMENT

This work has been supported in part by the National Science and Technology Major Project (Grant No. 2017ZX03001016), the National Natural Science Foundation of China (NSFC) Project (Grant Nos. 61571058 and 61601052), and the China State Grid Corp Science and Technology Project (5210ED180047), and State Key Laboratory of Advanced Optical Communication Systems Networks, China.

REFERENCES

[1] Z. Zhong, N. Hua, M. Tornatore, Y. Li, H. Liu, C. Ma, Y. Li, X. Zheng, and B. Mukherjee, "Energy efficiency and blocking reduction for tidal traffic via stateful grooming in IP-over-optical networks," *J. Opt. Commun. Netw.*, vol. 8, no. 3, pp. 175–189, 2016.

[2] Y. Zhao, B. Chen, J. Zhang, and X. Wang, "Energy efficiency with sliceable multi-flow transponders and elastic regenerators in survivable virtual optical networks," *IEEE Trans. Commun.*, vol. 64, no. 6, pp. 2539–2550, Apr. 2016.

[3] "Cisco Visual Networking Index: The zettabyte era: trends and analysis," Cisco White Paper [Online]. Available: https://www.cisco.com/c/en/us/solutions/collateral/service-provider/visual-networking-index-vni/vni-hyperconnectivity-wp.pdf.

[4] "Cisco Visual Networking Index: Global mobile data traffic forecast update, 2016-2021," Cisco White Paper [Online]. Available: https://www.cisco.com/c/en/us/solutions/collateral/service-provider/visual-networking-index-vni/mobile-white-paper-c11-520862.html.

[5] R. Li, Z. Zhao, X. Zhou, and H. Zhang, "Energy savings scheme in radio access networks via compressive sensing-based traffic load prediction," *Trans. Emerging Telecommun. Technol.*, vol. 25, no. 4, pp. 468–478, 2014.

[6] S. Sun, L. Gong, B. Rong, and K. Lu, "An intelligent SDN framework for 5G heterogeneous networks," *IEEE Commun. Mag.*, vol. 53, no. 11, pp. 142–147, 2015.

[7] S. Troia, G. Sheng, R. Alvizu, G. A. Maier, and A. Pattavina, "Identification of tidal-traffic patterns in metro-area mobile networks via matrix factorization based model," in *IEEE Int. Conf. on Pervasive Computing and Communications Workshops (PerCom Workshops)*, Kona, Hawaii, 2017, pp. 297–301.

[8] R. Alvizu, X. Zhao, G. Maier, Y. Xu, and A. Pattavina, "Energy efficient dynamic optical routing for mobile metro-core networks under tidal traffic patterns," *J. Lightwave Technol.*, vol. 35, no. 2, pp. 325–333, 2017.

[9] R. Alvizu, S. Troia, G. Maier, and A. Pattavina, "Matheuristic with machine-learning-based prediction for software-defined mobile metro-core networks," *J. Opt. Commun. Netw.*, vol. 9, no. 9, pp. D19–D30, 2017.

[10] M. Klinkowski, M. Ruiz, L. Velasco, D. Careglio, V. Lopez, and J. Comellas, "Elastic spectrum allocation for time-varying traffic in flexgrid optical networks," *IEEE J. Sel. Areas Commun.*, vol. 31, no. 1, pp. 26–38, 2013.

[11] B. H. Ramaprasad, T. Schöndienst, and V. M. Vokkarane, "Dynamic continuous and non-continuous advance reservation in SLICE networks," in *IEEE Int. Conf. on Communications (ICC)*, Sydney, NSW, Australia, 2014, pp. 3319–3324.

[12] B. C. Chatterjee, N. Sarma, and E. Oki, "Routing and spectrum allocation in elastic optical networks: a tutorial," *IEEE Commun. Surv. Tutorials*, vol. 17, no. 3, pp. 1776–1800, 2015.

[13] V. Lopez and L. Velasco, *Elastic Optical Networks Architectures Technologies and Control*, Springer, 2016, Chap. 4.

[14] K. Christodoulopoulos, I. Tomkos, and E. Varvarigos, "Elastic bandwidth allocation in flexible OFDM-based optical networks," *J. Lightwave Technol.*, vol. 29, no. 9, pp. 1354–1366, 2011.

[15] M. Jinno, B. Kozicki, H. Takara, A. Watanabe, Y. Sone, T. Tanaka, and A. Hirano, "Distance-adaptive spectrum resource allocation in spectrum-sliced elastic optical path network," *IEEE Commun. Mag.*, vol. 48, no. 8, pp. 138–145, 2010.

[16] A. N. Patel, P. N. Ji, J. P. Jue, and T. Wang, "Survivable transparent flexible optical WDM (FWDM) networks," in *Optical*

Fiber Communication Conf. and Exposition and the National Fiber Optic Engineers Conf., Los Angeles, California, 2011, paper OTuI2.

[17] A. N. Patel, P. N. Ji, J. P. Jue, and T. Wang, "Routing, wavelength assignment, and spectrum allocation algorithms in transparent flexible optical WDM networks," *Opt. Switching Netw.*, vol. 9, no. 3, pp. 191–204, 2012.

[18] T. Takagi, H. Hasegawa, K. I. Sato, Y. Sone, A. Hirano, and M. Jinno, "Disruption minimized spectrum defragmentation in elastic optical path networks that adopt distance adaptive modulation," in *37th European Conf. and Exhibition on Optical Communication*, Geneva, Switzerland, 2011, paper Mo.2.K.3.

[19] Z. Niu, "Tango: traffic-aware network planning and green operation," *IEEE Wireless Commun.*, vol. 18, no. 5, pp. 25–29, 2011.

[20] R. Alvizu, X. Zhao, G. Maier, Y. Xu, and A. Pattavina, "Energy aware optimization of mobile metro-core network under predictable aggregated traffic patterns," in *IEEE Int. Conf. on Communications (ICC)*, Kuala Lumpur, Malaysia, 2016.

[21] A. P. Vela, A. Vía, F. Morales, M. Ruiz, and L. Velasco, "Traffic generation for telecom cloud-based simulation," in *18th Transparent Optical Networks (ICTON)*, Trento, Italy, 2016, paper We.B3.2.

[22] J. Y. Yen, "Finding the k shortest loopless paths in a network," *Manage. Sci.*, vol. 17, no. 11, pp. 712–716, 1971.

[23] E. Bouillet, "Yen's K-Shortest Path Algorithm," in *Path Routing in Mesh Optical Networks*, Wiley, 2007, Chap. 6.3.1.

[24] M. L. Fredman and R. E. Tarjan, "Fibonacci heaps and their uses in improved network optimization algorithms," *J. ACM*, vol. 34, no. 3, pp. 596–615, 1987.

Boyuan Yan received his B.E. in Communication Engineering from Beijing University of Posts and Telecommunications (BUPT) in 2015. He is currently pursuing a Ph.D. at BUPT. His research interests include software defined optical networking, service function chaining, and network resource allocation with machine learning.

Yongli Zhao is currently an associate professor at the Institute of Information Photonics and Optical Communications (IPOC) at Beijing University of Posts and Telecommunications (BUPT). He received a B.S. in Communication Engineering and a Ph.D. in Electromagnetic Field and Microwave Technology from BUPT, respectively, in 2005 and in 2010. He has published more than 150 journal and conference articles. His research focuses on software defined optical networks, flexi-grid optical networks, network virtualization, and so on.

Xiaosong Yu received his Ph.D. from Beijing University of Posts and Telecommunications (BUPT), Beijing, China in 2015, and was a visiting scholar at the University of California, Davis from Sep. 2013 to Sep. 2014. Now he is an assistant professor at the Institute of Information Photonics and Optical Communications (IPOC) in BUPT. To date, he has co-authored more than 50 international journal and conference papers. His research focuses on spatial division multiplexing enabled elastic optical networks (SDM-EONs), software defined optical networking (SDON), datacenter networking, and optical network security.

Wei Wang received his B.S. in Communication Engineering from Beijing University of Posts and Telecommunications (BUPT), in 2013. He is currently working toward a Ph.D. in Information and Communications Engineering at BUPT. He is now a visiting research scholar at the University of California, Davis. His research interests include software defined networking, network function virtualization, and mobile edge computing.

Yu Wu received his B.E. in Information and Communication Engineering from Zhejiang University, Zhejiang, China, in 2014. He is currently pursuing a Ph.D. in the Computer Science Department at the University of California Davis. His research interests include cloud and optical network resource management, green energy communication, and 5G emerging technologies.

Ying Wang received her Ph.D. in Information and Communication Engineering from Beijing University of Posts and Telecommunications (BUPT) in 2012. More than 20 journal and conference articles have been published. Her research focuses on electronic communication networks, green energy communication, machine learning, etc.

Jie Zhang is currently a professor and the vice dean of Information Photonics and Optical Communications Institute at Beijing University of Posts and Telecommunications (BUPT), China. He received his bachelors degree in Communication Engineering and a Ph.D. in Electromagnetic Field and Microwave Technology from BUPT. He has published more than 300 technical papers, authored eight books, and submitted 17 ITU-T recommendation contributions and six IETF drafts. He also holds 17 patents. He has served as a TPC member for a number of conferences, such as ACP, OECC, PS, ONDM, COIN, and ChinaCom. His research focuses on the architecture, protocols, and standards of optical transport networks.